

RESEARCH ARTICLE

Novel coating containing molybdenum oxide nanoparticles to reduce *Staphylococcus aureus* contamination on inanimate surfaces

Susana Piçarra^{1,2}, Elizeth Lopes³, Pedro L. Almeida^{4,5}, Hermínia de Lencastre^{3,6}, Marta Aires-de-Sousa^{3,7}*

1 Centro de Química Estrutural-CQE, DEQ, Instituto Superior Técnico, Universidade de Lisboa, Lisboa, Portugal, **2** Escola Superior de Tecnologia do Barreiro, Instituto Politécnico de Setúbal, Rua Américo da Silva Marinho, Lavradio, Portugal, **3** Laboratory of Molecular Genetics, Instituto de Tecnologia Química e Biológica António Xavier (ITQB), Universidade Nova de Lisboa (UNL), Oeiras, Portugal, **4** CENIMAT/I3N, Departamento de Ciência dos Materiais, Faculdade de Ciências e Tecnologia (FCT), Universidade Nova de Lisboa (UNL), Caparica, Portugal, **5** Área Departamental de Física, Instituto Superior de Engenharia de Lisboa (ISEL) Instituto Politécnico de Lisboa (IPL), Lisboa, Portugal, **6** Laboratory of Microbiology and Infectious Diseases, The Rockefeller University, New York, United States of America, **7** Escola Superior de Saúde da Cruz Vermelha Portuguesa (ESSCVP), Lisboa, Portugal

☞ These authors contributed equally to this work.

* msousa@esscvp.eu



OPEN ACCESS

Citation: Piçarra S, Lopes E, Almeida PL, de Lencastre H, Aires-de-Sousa M (2019) Novel coating containing molybdenum oxide nanoparticles to reduce *Staphylococcus aureus* contamination on inanimate surfaces. PLoS ONE 14(3): e0213151. <https://doi.org/10.1371/journal.pone.0213151>

Editor: Yogendra Kumar Mishra, Institute of Materials Science, GERMANY

Received: November 14, 2018

Accepted: February 17, 2019

Published: March 18, 2019

Copyright: © 2019 Piçarra et al. This is an open access article distributed under the terms of the [Creative Commons Attribution License](https://creativecommons.org/licenses/by/4.0/), which permits unrestricted use, distribution, and reproduction in any medium, provided the original author and source are credited.

Data Availability Statement: All relevant data are within the manuscript.

Funding: This work was partly supported by projects PTDC/DTP-EPI/0842/2014, PTDC/FIS/NAN/0117/2014, LISBOA-01-0145-FEDER-007660 (Microbiologia Molecular, Estrutural e Celular), UID/CTM/50025/2013 and UID/UI/00100/2019 funded by FEDER funds through COMPETE2020 - Programa Operacional Competitividade e Internacionalização (POCI) and by national funds

Abstract

We previously synthesized molybdenum oxide (MoO₃) nanoparticles (NP) and showed their antibacterial activity against a representative collection of the most relevant bacterial species responsible for hospital-acquired infections, including *Staphylococcus aureus*. The aim of the present study was to prepare and characterize a novel coating with these MoO₃ NP, confirm its mechanical stability, and investigate its biocidal effect to reduce *S. aureus* contamination on inanimate surfaces. In addition, the novel MoO₃ NP coating was compared to a silver (Ag) NP coating synthesized by the same procedure. The MoO₃ and Ag NP coatings were characterized in terms of their chemical structure by FT-IR, surface morphology by scanning electron microscopy, and mechanical properties by tensile and adhesion tests. The antimicrobial activity of the coatings was tested by following the loss of viability of *S. aureus* after 6h, 24h, 48h, and 72h exposure. MoO₃ and Ag coatings exhibited surfaces of comparable morphologies and both presented elastomeric properties (tensile strength of ~420 kPa, Young's modulus of ~48 kPa, and maximum elongation of ~12%), and excellent (classification of 5B) adhesion to glass, steel and polystyrene surfaces. The two coatings exhibited a good antibacterial activity (R) against *S. aureus* over time (R_{MoO₃} = 0.2–0.81; R_{Ag} = 0.61–2.37), although the effect of the Ag NP coating was more pronounced, especially at 72h (R_{MoO₃} = 0.81 vs R_{Ag} = 2.37). Noteworthy, contrary to the Ag NP coating, the MoO₃ NP coating was colourless and transparent, avoiding undesired unaesthetic effects. The synthesized coating with NP of MoO₃, which has low toxicity to humans, capability of biodegradation, and rapid excretion, can be applied onto most standard materials and therefore is a promising tool to reduce *S. aureus* contamination on usual inanimate surfaces found in healthcare and community environments.

through Fundação para a Ciência e a Tecnologia (FCT), Portugal. Elizeth Lopes was supported by grant 03/BI/2017 from (FCT), Portugal.

Competing interests: The authors have declared that no competing interests exist.

Introduction

Staphylococcus aureus remains a leading cause of bacterial infections worldwide, ranging from skin and soft tissue infections to more severe conditions such as bacteremia, meningitis, pneumonia, osteomyelitis, and endocarditis. The high morbidity and mortality associated to *S. aureus* infections is due largely to its methicillin resistant form (MRSA), which was historically associated exclusively with hospital-acquired infections, but subsequently spread also to the community posing new threats and challenges.

S. aureus is able to survive on a variety of environmental surfaces, over a wide range of temperatures, humidity, and exposure to sunlight promoting contamination of inanimate surfaces [1]. Therefore, although transmission of *S. aureus* occurs mainly by direct human-to-human skin contact, environmental surfaces represent an important reservoir for dissemination as well.

We have shown that public transportation constitutes an indubitable reservoir of MRSA and a transmission route from the hospital to the community [2, 3]. It is also well known that hospital environmental surfaces represent a source of infection and colonization for patients and healthcare workers. Therefore, efficient measures to reduce *S. aureus* environmental surfaces contamination are urgently needed in the healthcare system and in the community.

Nanostructure materials have gained increased attention in the biomedical field due to their antimicrobial activity in low concentrations [4]. Out of the different nanomaterials considered for their antibacterial properties, silver (Ag) nanoparticles (NP) have been extensively studied since they possess remarkable broad-spectrum antimicrobial capacities [5, 6]. However, the high cost of silver and the toxicity of Ag NP limits its applications [7].

The antibacterial action of Ag NP has been mainly attributed to the action of Ag⁺ ions in membrane disruption, generation of reactive oxygen species (ROS) stress and genotoxic damage, which leads to cell death [8]. The ROS production has been recently linked to the interaction of Ag NP with different cellular proteins [9, 10]. However, the bactericidal effect of MoO₃ NP has been attributed to the release of hydronium ions affecting enzyme activity, protein stability, and structure of nucleic acids, thus killing the bacteria [11]. We have previously synthesized pure molybdenum oxide (MoO₃) NP, a non-toxic compound, and recently showed their antibacterial activity against a representative collection of the most relevant bacterial species responsible for hospital-acquired infections, including *S. aureus* [12].

The aim of the present study was to prepare and characterize a novel coating with these MoO₃ NP, confirm its mechanical stability, and investigate its biocidal effect to reduce *S. aureus* contamination on inanimate surfaces. In addition, the novel MoO₃ NP coating will be compared to a Ag NP coating synthesized by the same procedure.

Methods

Synthesis of MoO₃ and Ag NP coatings

MoO₃ NP (Sigma-Aldrich, St. Louis, MO, USA) were prepared following the one-step thermal decomposition approach using ammonium heptamolybdate tetrahydrate [(NH₄)₆Mo₇O₂₄·4H₂O] (Chem-Lab NV, Zedelgem, Belgium) as starting precursor, for 4h at 500°C [12]. Ag NP (purity 99.5%; Sigma-Aldrich, St. Louis, MO, USA) and N1-(3-trimethoxysilylpropyl)diethylenetriamine (SiDETA) (technical grade, Sigma-Aldrich, St. Louis, MO, USA) were used as received.

NP coatings of MoO₃ and Ag (MoO₃CT and AgCT) were prepared by dispersing 0.118 mmol of NP (0.085 g for MoO₃; 0.0637g for Ag) into 50 ml of ethanol (EtOH). After 20 min of sonification, 50 µl of SiDETA was added, during stirring. A coating without NP (CT) was also prepared, directly from a 1.9 mM solution of SiDETA in EtOH.

Films from the three above described coatings (CT, AgCT and MoO₃CT) were prepared on different substrates (glass, polystyrene and steel AA2024) by dip coating (three dives with ascending/descending movements of 5 s), spraycoating (three sprays of 5 s each), and by brush (painted twice with 15 minutes break between them).

Morphologic and chemical characterization of MoO₃ and Ag NP coatings

The morphology of the films deposited by dip coating was assessed by using a scanning electron microscope CrossBeam Workstation (SEM-FIB)–Zeiss Auriga. The SEM images under the in-lens mode were carried out with an acceleration voltage of 2 kV and aperture size of 30 μm. A thin carbon layer (< 20 nm) was deposited on the suspended fibers using a Q150T ES Quorum sputter coater.

Coatings chemical structure was unveiled by FT-IR. The FT-IR data were obtained using an Attenuated Total Reflectance (ATR) sampling accessory (Smart iTR) equipped with a single bounce diamond crystal on a Thermo Nicolet 6700 Spectrometer. The spectra were acquired with a 45° incident angle in the range of 4000–600 cm⁻¹ and with a 4 cm⁻¹ resolution.

Tensile and adhesion tests

Mechanical tensile tests were performed on samples from the three coatings. In order to have free standing films to do the tensile tests, the films were allowed to set on a Teflon mould. From the obtained films (with thicknesses of around 50 μm), test specimens were cut with the dimensions of 15x30 mm², leaving after assembly a distance between clamps (*l*₀) of 10 mm. The tensile test machine used was Rheometric Scientific (Minimat–Firmware V. 3.1) testing machine. The measurements were carried out at room temperature (25°C). Five successful determinations were used to obtain average values. The stretching rate was 5 mm/min. The stress, σ , was determined in terms of the original cross-sectional area (*A*₀), and the strain defined as $\epsilon = (l - l_0)/l_0$, where *l* and *l*₀ are the length at the time of data collection and original length, respectively.

The three produced coatings were tested for their adhesion to different substrates according to the American Society for Testing and Materials Standard D3359-17: “Standard Test Methods for Rating Adhesion by Tape Test” [13]. In the Standard, two testing methods are defined A and B. Test method B is more suitable for use in laboratory environment, having the limitation of the coating thickness not to exceed 125 μm. Three substrates (polystyrene, steel and glass) were used for the adhesion testing coated with CT, MoO₃CT and AgCT, with a thickness under 100 μm after solvent evaporation. The adhesion tests were performed in triplicate for each sample.

Antimicrobial activity of the MoO₃ NP coating

A bacterial suspension (100 μl) of *S. aureus* strain ATCC25923 adjusted to 0.5 McFarland was spread on sterilized microscope glasses covered with the coating with MoO₃ NP and on glasses with the coating without NP (control). After drying the glasses were scrubbed with a swab moistened in sterile water that was subsequently inserted into 1 ml H₂O and vortexed for 1 minute. Serial dilutions were inoculated onto Tryptic Soy Agar (TSA, Becton, Dickinson & Co, New Jersey, USA) plates which were incubated at 37°C overnight (ON). The same procedure was repeated for 6 h, 24 h, 48 h and 72 h.

The antimicrobial activity (*R*) of the MoO₃ NP coating was calculated using the following equation:

$$R = (A_0 - A_t) - (C_0 - C_t) \quad (1)$$

where A and C are the common logarithm of the number of viable cells recovered from the surfaces covered with the coating with NP (A) and from the surfaces covered with the coating without NP (C-control) immediately after inoculation (A₀ and C₀) and after each incubation time (A_t and C_t).

The experiments were performed in triplicate and the antimicrobial activity was calculated with the average colony forming units (CFU) counts.

Comparison of the antimicrobial activity of the MoO₃ and Ag NP coatings

Considering the well-known antibacterial properties of silver, we additionally evaluated the antimicrobial activity of the synthesized Ag NP coating against *S. aureus* for comparison of the biocidal effect of the MoO₃ NP coating. We performed the assay as above, with microscope glasses covered with coatings with Ag NP using three different concentrations (Ag_{100%}—same NP concentration used for the MoO₃ NP coating [2.36 mM], Ag_{50%}—half NP concentration [1.18 mM], and Ag_{25%}—one quarter NP concentration [0.59 mM]). The antimicrobial activity was calculated as above.

Results and discussion

Synthesis of MoO₃ and Ag NP coatings

SiDETA is an ORMOSIL compound composed by a head containing three alkoxy groups and by an organic tail containing three amino groups (Fig 1). In the presence of water (from EtOH solution and from atmospheric moisture), alkoxy groups from the SiDETA head suffer hydrolysis and condensation through the very well-known sol-gel process, originating a silica network that constitutes the coating (and water and methanol as byproducts) [14, 15]. This process is, however, very much dependent on the reactional medium conditions (temperature, moisture, pH, etc.) and the introduction of Ag or MoO₃ NP might result in networks with distinct structures, originating coatings with distinct properties. All synthesis were made under atmospheric pressure and at 20±5°C. SiDETA pH was 10.88 ± 0.49, which remained stable after the induction of NP.

Characterization of MoO₃ and Ag NP coatings

The SEM-FIB images of MoO₃ and Ag NP showed that both NP present 2D plate-like morphologies (Ag NP showing rougher surfaces than MoO₃ NP) with average dimensions of 200–800 nm and 50–200 nm, respectively (Fig 2A and 2B). SEM-FIB images of the produced SiDETA coatings showed that while the CT surfaces are smooth (Fig 2C and 2F), MoO₃CT (Fig 2D and 2G) and AgCT (Fig 2F and 2H) surfaces are rough, showing aggregates of NP of

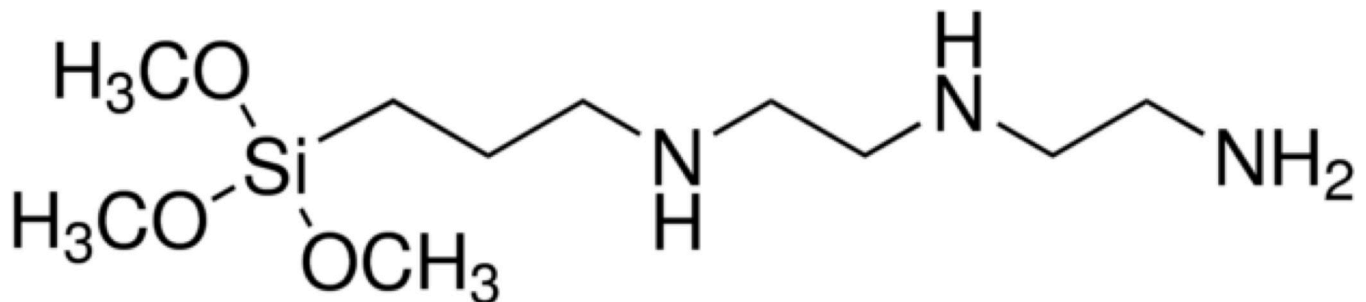


Fig 1. Molecular structure of N1-(3-trimethoxysilylpropyl)diethylenetriamine (SiDETA).

<https://doi.org/10.1371/journal.pone.0213151.g001>

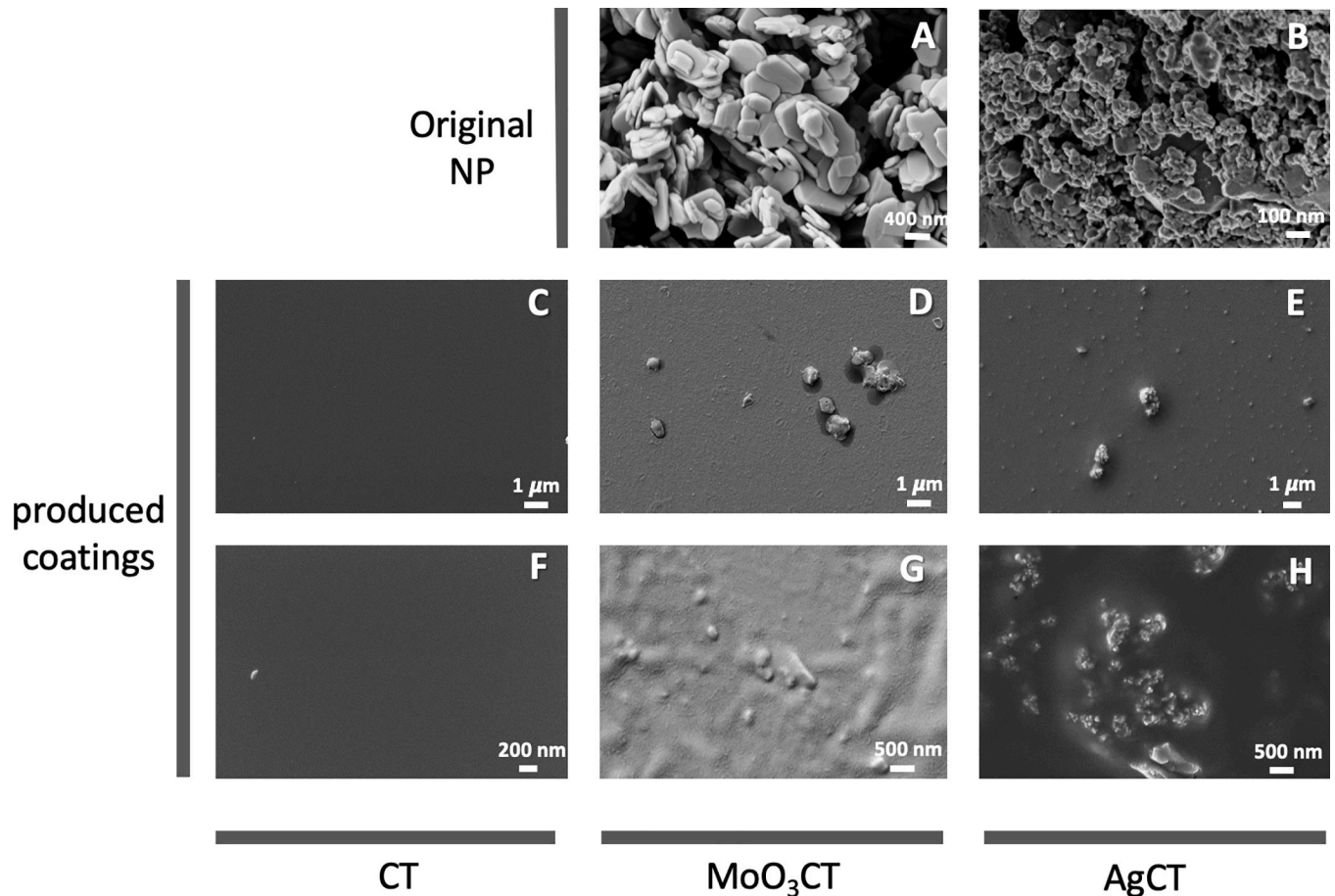


Fig 2. SEM-FIB images of the MoO₃ and Ag NP (A and B, respectively) and the produced coatings; CT (C and F), MoO₃CT (D and G), and AgCT (E and H).

<https://doi.org/10.1371/journal.pone.0213151.g002>

similar dimensions (0.5 to 1.0 μm), independently of the individual dimensions of the MoO₃ and Ag NP.

The FT-IR spectra of the three coatings (CT, MoO₃CT, and AgCT) are, however, quite similar (Fig 3), all spectra revealing the characteristic patterns of a silica network and amine and methylene groups.

From the FT-IR spectra it is possible to conclude that independently of the presence of MoO₃ and Ag NP, the alkoxy silane groups of SiDETA *head* had suffered similar sol-gel reactions and formed networks with similar chemical bounds. We could also observe that the organic amine groups containing *tail* remained in the formed network, as expected. The presence of the organic *tail* should be responsible for introducing elasticity into the resulting coating material and the amino groups to increase the coating adhesion properties.

Therefore, the three produced coatings (CT, MoO₃CT and AgCT) were tested for their adhesion to different substrates (polystyrene, steel and glass) [13]. All samples obtained an adhesion classification of 5B according to the standard classification which means that the edges of the cuts are completely smooth; none of the squares of the cut lattice was detached. These adhesion assays proved that the coatings (with and without NP) have a strong adhesion to the tested substrates and therefore are suitable to coat most standard materials and therefore suitable for usual surfaces found in healthcare and community environments.

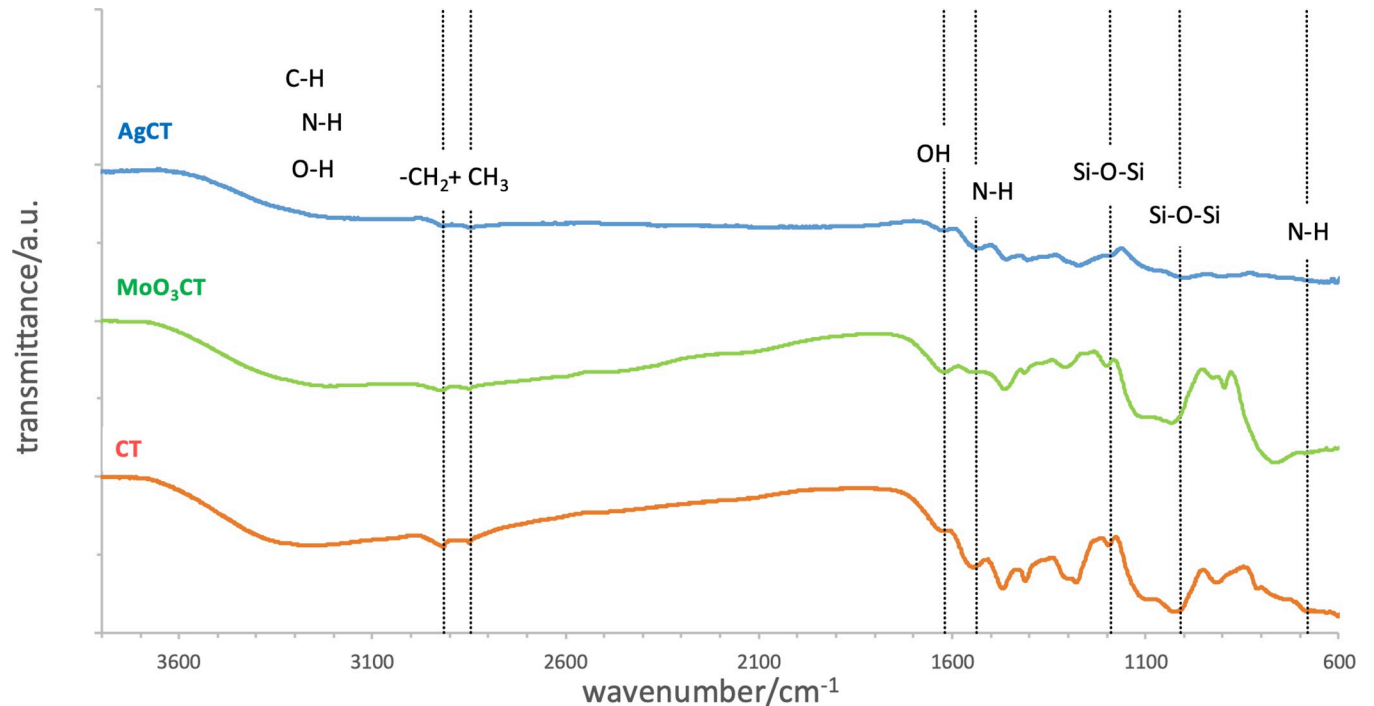


Fig 3. FT-IR spectra of the three coatings (CT, MoO₃CT, and AgCT).

<https://doi.org/10.1371/journal.pone.0213151.g003>

Mechanical tensile tests were additionally performed on samples from the three coatings. The tensile stress–strain curves, for the range of weight ratios (HPC/BDI) studied, did not exhibit a yield point. The tensile strength, the elongation, and the Young's modulus did not change significantly between samples indicating that the presence of MoO₃ and Ag nanoparticles does not affect the mechanical behavior of the formed networks that constitute the coatings. These coatings mechanically behave as rigid elastomers presenting a tensile strength of around 420 kPa, a Young's modulus of around 48 kPa and a maximum elongation of around 12%. The determined mechanical properties clearly state that these materials are suitable for this application [16], presenting mechanical robustness that allows the coating to resist to its practical usage.

While Ag NP containing coating is visually aesthetical (black and opaque) which limits several applications, MoO₃ NP are colorless and transparent, being suitable to be applied on a diversity of surfaces in both clinical and community settings (Fig 4).

Antimicrobial activity of the MoO₃ and Ag NP coatings

The results demonstrated that the synthesized MoO₃ NP coating exhibited antibacterial activity against *S. aureus*, in a time-dependent way until 48 h of contact time (Fig 5). Noteworthy, the biocidal effect of the MoO₃ NP coating was also verified after 28 days indicating its long-term stability on glass surfaces (results not shown).

Considering the well-known antibacterial properties of silver, we prepared a coating containing Ag NP as a positive control, using the same procedure and the same amount of NP (Ag_{100%}). When comparing the antibacterial activity of the MoO₃ and the Ag_{100%} NP coatings towards *S. aureus*, under the same conditions, the former showed a lower antibacterial activity (Fig 5). Nevertheless, the MoO₃ NP coating reached 58% and 80% of the biocidal effect of the Ag_{100%} NP coating at 24 h and 48 h, respectively (Fig 6A). Remarkably, the antimicrobial

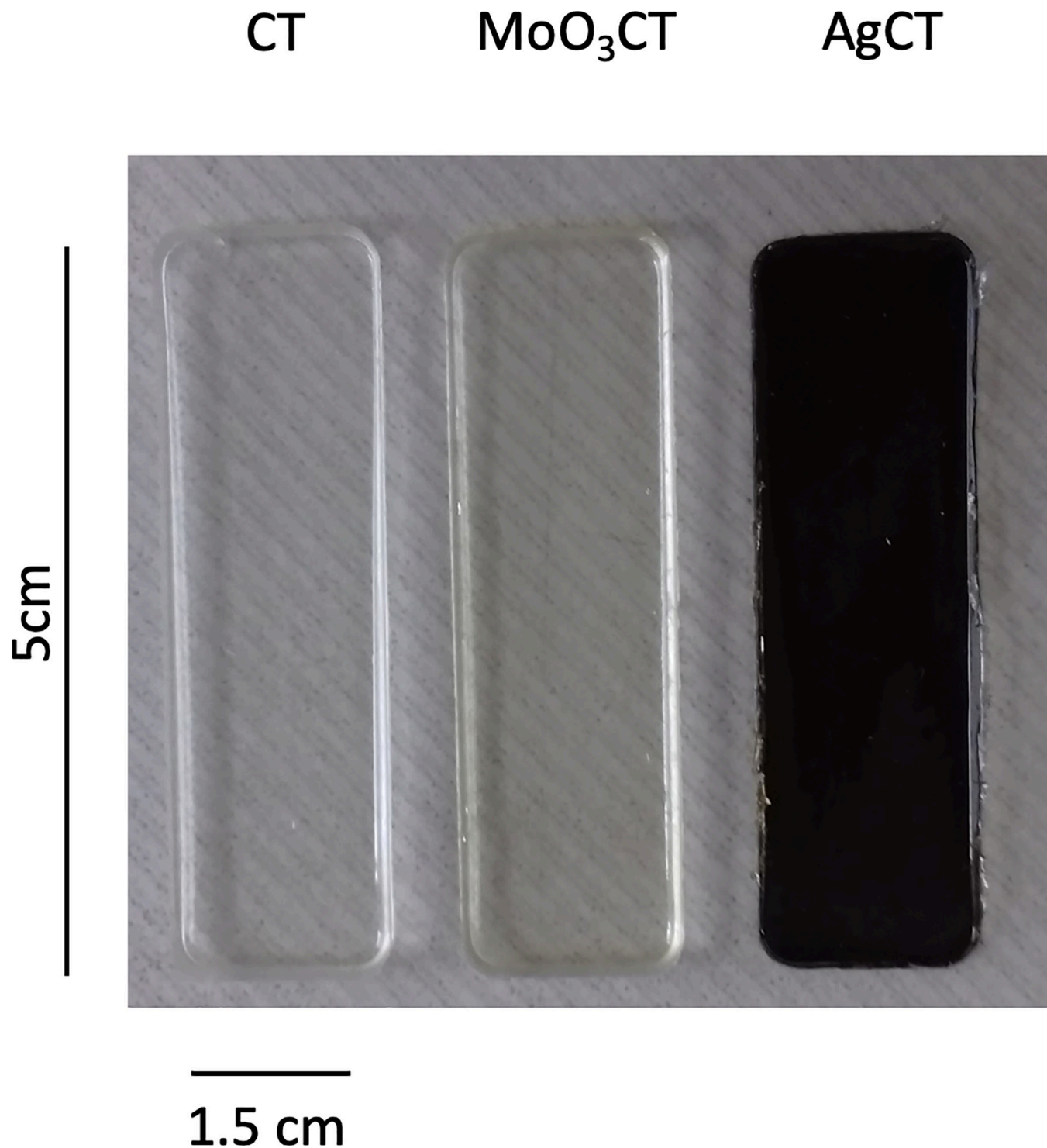


Fig 4. Digital photographs of microscope glasses covered with the three coatings (CT, MoO₃CT, and AgCT).

<https://doi.org/10.1371/journal.pone.0213151.g004>

efficacy was slower for the MoO₃ NP coating, since after 6 h of contact it reached just one third of the Ag_{100%} NP effect and lasted for a shorter period of time showing only 11% of the effect of the Ag_{100%} NP at 72 h (Fig 6A).

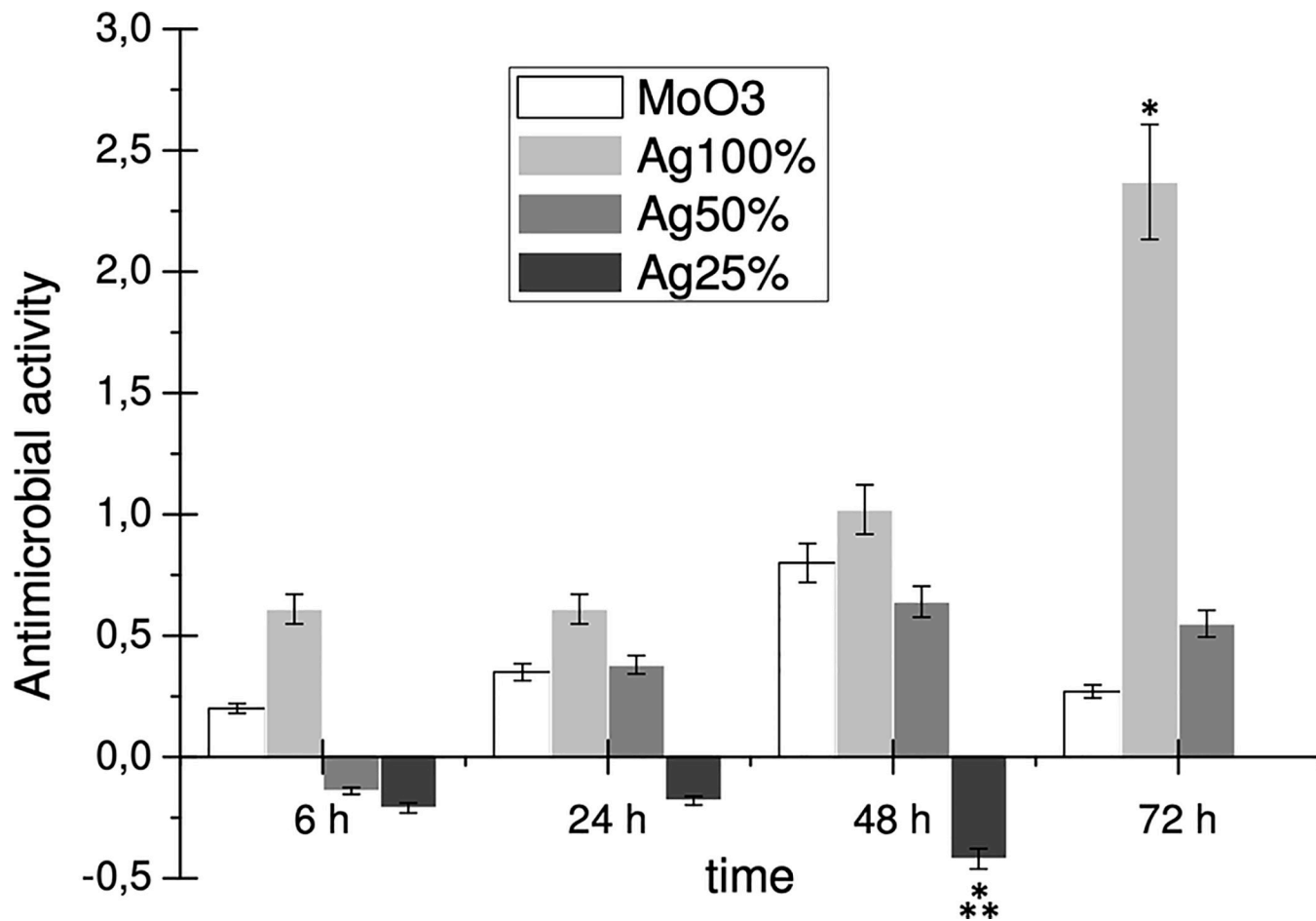


Fig 5. Antimicrobial activity of MoO₃ and Ag NP coatings against *S. aureus* strain ATCC25923. * and ** denote significant change ($p < 0.05$) compared to MoO₃ and Ag100, respectively.

<https://doi.org/10.1371/journal.pone.0213151.g005>

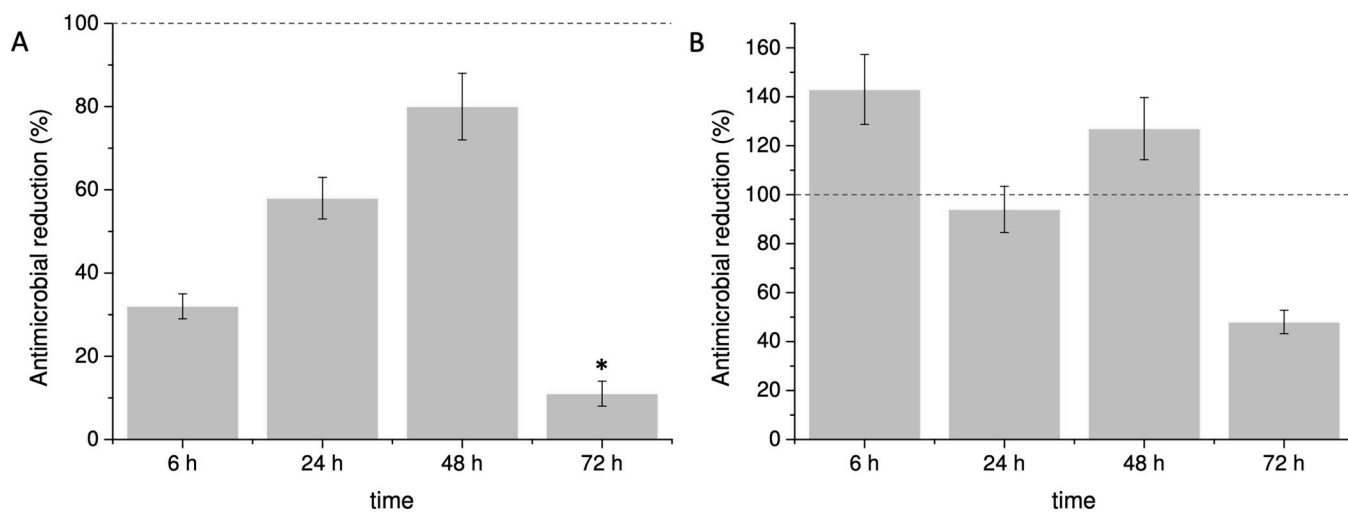


Fig 6. Comparison of the antibacterial effect of the MoO₃ NP coating with two Ag NP coatings: A) Ag_{100%}—same NP concentration used for the MoO₃ NP coating; B) Ag_{50%}—half NP concentration. * denotes significant change ($p < 0.05$).

<https://doi.org/10.1371/journal.pone.0213151.g006>

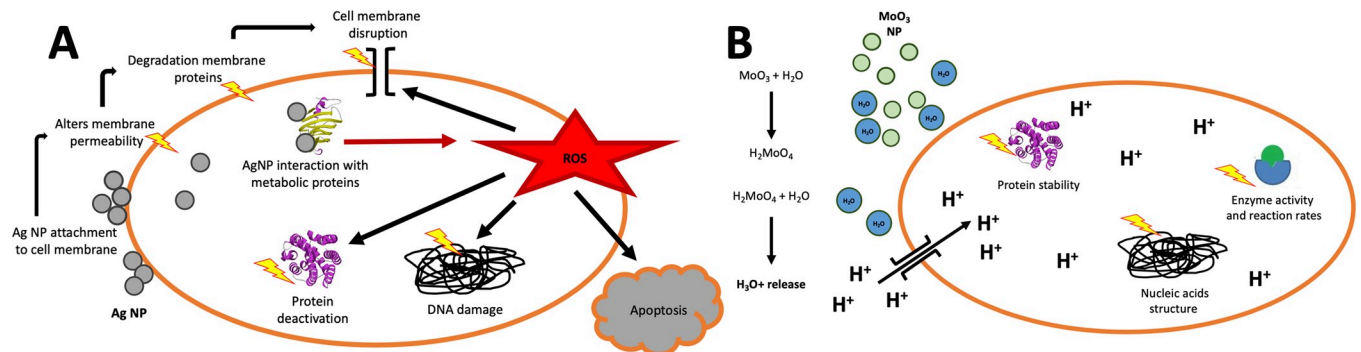


Fig 7. Schematic diagram of the mechanism of antimicrobial action of Ag (A) and MoO₃ (B) NP.

<https://doi.org/10.1371/journal.pone.0213151.g007>

Decreasing the Ag NP concentration on the coating resulted in a decreased antimicrobial activity, and when the NP concentration was reduced to 25%, the biocidal effect was totally abolished (Fig 5). The results showed that the MoO₃ coating was at least as efficient as the Ag_{50%} NP coating until 48 h of contact, showing a much faster biocidal effect for 6 h and even an increased efficacy at 48 h (Fig 6B).

The differences observed in the antimicrobial effectivity of the MoO₃ and Ag coatings might be due to the different modes of action of the NP (Fig 7). The Ag NP act as an antimicrobial by a combination of several mechanisms: (i) adhesion to the bacterial cell wall, followed by penetration, causing structural alterations in the cell membrane and subsequent death of the bacteria, (ii) formation of free radicals by the Ag NP which damage the cell membrane leading to cell death, (iii) release of silver ions (Ag⁺) which inactivate several vital enzymes and inhibit numerous functions in the cell, and (iv) generation of reactive oxygen species (ROS), that damage DNA and mitochondria, cause oxidation of proteins and lipids, cell membrane disruption and activate apoptosis [17–19]. In contrast, the antibacterial effect of the MoO₃ NP is due to the creation of an acidic environment by conversion of MoO₃ into molybdic acid (H₂MoO₄) and subsequent release of H₃O⁺ ions, which requires the presence of water. The hydronium ions diffuse into the cell membranes affecting enzyme activity and reaction rates, protein stability, and structure of nucleic acids, thus killing the bacteria [11]. Therefore, when embedding the MoO₃ NP in the coating, the interaction with water is restricted to the contact time with the aqueous bacterial suspension, which might explain the pronounced reduction in the antibacterial activity at 72h (the surface has considerably dried) as well as a less pronounced antimicrobial effect compared to the NP in an aqueous solution, as previously shown [12].

An effective antimicrobial coating must include several characteristics: (i) be able to reduce the pathogenic population on a surface; (ii) be stable (mechanically and chemically); (iii) minimize toxicological effects and risks of emergence of antimicrobial resistance; (iv) be affordable and easily implemented [20]. The MoO₃ NP coating synthesized in the current study is mechanically and chemically stable, presented rigid elastomeric properties, exceptional adhesion to glass, steel and polystyrene surfaces, and has proved to be able to control a *S. aureus* population on a surface. Moreover, molybdenum has low toxicity to humans, capability of biodegradation, and rapid excretion [21], and to the best of our knowledge bacterial resistance to MoO₃ NP has not been described so far. In addition, Ag NP containing coating is visually unaesthetic which limits several applications, while MoO₃ is colorless and transparent.

In conclusion, we synthesized a novel MoO₃ NP coating using an easy and timesaving protocol. The characterization of the coating showed it can be applied onto most standard materials, it has antimicrobial activity against *S. aureus*, and therefore is suitable to reduce bacterial contamination on usual surfaces found in healthcare and community environments.

Acknowledgments

We thank Dr. Bruno Sena da Fonseca for helpful discussions.

Author Contributions

Conceptualization: Susana Piçarra, Pedro L. Almeida, Marta Aires-de-Sousa.

Funding acquisition: Marta Aires-de-Sousa.

Investigation: Elizeth Lopes.

Project administration: Marta Aires-de-Sousa.

Supervision: Susana Piçarra, Marta Aires-de-Sousa.

Writing – original draft: Marta Aires-de-Sousa.

Writing – review & editing: Susana Piçarra, Pedro L. Almeida, Hermínia de Lencastre, Marta Aires-de-Sousa.

References

1. Dancer SJ Importance of the environment in meticillin-resistant *Staphylococcus aureus* acquisition: the case for hospital cleaning. *Lancet Infect Dis* 2008; 8: 101–13. [https://doi.org/10.1016/S1473-3099\(07\)70241-4](https://doi.org/10.1016/S1473-3099(07)70241-4) PMID: 17974481
2. Conceicao T, Diamantino F, Coelho C, de Lencastre H, Aires-de-Sousa M Contamination of public buses with MRSA in Lisbon, Portugal: A possible transmission route of major MRSA clones within the community. *Plos One* 2013; 8.
3. Simoes RR, Aires-de-Sousa M, Conceicao T, Antunes F, da Costa PM, de Lencastre H High prevalence of EMRSA-15 in Portuguese public buses: A worrisome finding. *Plos One* 2011; 6.
4. Hajipour MJ, Fromm KM, Ashkarran AA, de Aberasturi DJ, de Larramendi IR, Rojo T, et al. Antibacterial properties of nanoparticles. *Trends Biotechnol* 2012; 30: 499–511. <https://doi.org/10.1016/j.tibtech.2012.06.004> PMID: 22884769
5. Nanda A, Saravanan M Biosynthesis of silver nanoparticles from *Staphylococcus aureus* and its antimicrobial activity against MRSA and MRSE. *Nanomed-Nanotechnol* 2009; 5: 452–6.
6. Taheri S, Cavallaro A, Christo SN, Smith LE, Majewski P, Barton M, et al. Substrate independent silver nanoparticle based antibacterial coatings. *Biomaterials* 2014; 35: 4601–9. <https://doi.org/10.1016/j.biomaterials.2014.02.033> PMID: 24630091
7. AshaRani PV, Mun GLK, Hande MP, Valiyaveetil S Cytotoxicity and Genotoxicity of silver nanoparticles in human cells. *Acs Nano* 2009; 3: 279–90. <https://doi.org/10.1021/nn800596w> PMID: 19236062
8. Verma SK, Jha E, Sahoo B, Panda PK, Thirumurugan A, Parashar SKS, et al. Mechanistic insight into the rapid one-step facile biofabrication of antibacterial silver nanoparticles from bacterial release and their biogenicity and concentration-dependent in vitro cytotoxicity to colon cells. *Rsc Adv* 2017; 7: 40034–45.
9. Paul P, Verma S, Kumar Panda P, Jaiswal S, Sahu BR, Suar M Molecular insight to influential role of Hha-TomB toxin-antitoxin system for antibacterial activity of biogenic silver nanoparticles. *Artif Cells Nanomed Biotechnol* 2018; <https://doi.org/10.1080/21691401.2018.1503598>: 1–13
10. Verma SK, Jha E, Panda PK, Thirumurugan A, Patro S, Parashar SKS, et al. Molecular insights to alkaline based bio-fabrication of silver nanoparticles for inverse cytotoxicity and enhanced antibacterial activity. *Mater Sci Eng C Mater Biol Appl* 2018; 92: 807–18. <https://doi.org/10.1016/j.msec.2018.07.037> PMID: 30184810
11. Zollfrank C, Gutbrod K, Wechsler P, Guggenbichler JP Antimicrobial activity of transition metal acid MoO₃ prevents microbial growth on material surfaces. *Mat Sci Eng C-Mater* 2012; 32: 47–54.
12. Lopes E, Picarra S, Almeida PL, de Lencastre H, Aires-de-Sousa M Bactericidal efficacy of molybdenum oxide nanoparticles against antimicrobial-resistant pathogens. *J Med Microbiol* 2018; 67: 1042–6. <https://doi.org/10.1099/jmm.0.000789>
13. ASTM. ASTM D3359-17 Standard Test Methods for Rating Adhesion by Tape Test. West Conshohocken, PA: ASTM International 2017.

14. da Fonseca BS, Picarra S, Pinto APF, Ferreira MJ, Montemor MF TEOS-based consolidants for carbonate stones: the role of N1-(3-trimethoxysilylpropyl)diethylene-triamine. *New J Chem* 2017; 41: 2458–67.
15. Brinker CJaSGW. *Sol-gel science: the physics and chemistry of sol-gel processing.*, 1st edn. San Diego: Academic Press 1990.
16. Merchan M, Sedlarikova J, Vesel A, Sedlarik V, Pastorek M, Saha P Characterization of antibacterial, mechanical, and structural properties of polyvinyl chloride/silver nitrate composites prepared by thermoplastic compounding. *International Journal of Polymer Analysis and Characterization* 2010; 15: 360–9.
17. Flores-Lopez LZA-Ohoo, Espinoza-Gomez HA-Ohoo, Somanathan R Silver nanoparticles: Electron transfer, reactive oxygen species, oxidative stress, beneficial and toxicological effects. Mini review. LID — <https://doi.org/10.1002/jat.3654> PMID: 29943411
18. Prabhu S, Poulouse EK Silver nanoparticles: mechanism of antimicrobial action, synthesis, medical applications, and toxicity effects. *International Nano Letters* 2012; 2: 32.
19. Verma SK, Jha E, Panda PK, Das JK, Thirumurugan A, Suar M, et al. Molecular aspects of core-shell intrinsic defect induced enhanced antibacterial activity of ZnO nanocrystals. *Nanomedicine (Lond)* 2018; 13: 43–68.
20. Adlhart C, Verran J, Azevedo NF, Olmez H, Keinanen-Toivola MM, Gouveia I, et al. Surface modifications for antimicrobial effects in the healthcare setting: a critical overview. *J Hosp Infect* 2018; 99: 239–49. <https://doi.org/10.1016/j.jhin.2018.01.018> PMID: 29410096
21. Hao JL, Song GS, Liu T, Yi X, Yang K, Cheng L, et al. In vivo long-term biodistribution, excretion, and toxicology of PEGylated transition-metal dichalcogenides MS₂ (M = Mo, W, Ti) nanosheets. *Adv Sci* 2017; 4.